PHYSICS AND CHEMISTRY OF SOLID STATE
V. 25, No. 1 (2024) pp. 73-78
Section: Physics

DOI: 10.15330/pcss.25.1.73-78

Vasyl Stefanyk Precarpathian National University

ФІЗИКА І ХІМІЯ ТВЕРДОГО ТІЛА
Т. 25, № 1 (2024) С. 73-78

Фізико-математичні науки

PACS: 31.90.+s; 71.15.Ap

ISSN 1729-4428

Sameen F. Mohammed, Mahmood A. Mohammed

A study electronic structure of InSb: Experiment and Theory

Department of Mechanical Techniques, Technical Institute Kirkuk, Northern Technical University, Iraq,
sameenmhammed@gmail.com

The current study shows the results related to investigating the Compton scattering (Cs) of Indium Antimonite (InSb). ^{241}Am with 59.54 keV Gamm-radiations source Compton spectrometer is employed for the purpose of experimental measurement. The linear combination of atomic orbitals -LCAO technique is utilised within the density functional theory -DFT framework to assess the theoretical values of distributing the electron momentum density. A comparison is then achieved in between the research findings and empirical data. The experimental isotropic profiles were in a relative agreement with the DFT data. Additionally, calculations employing the ionic model (IO) based on the 5p state of In and the 5p state of Sb atoms reveal that 0.5 electrons of the state of 5p In may have been transferred to the 5p state of Sb atoms in order to estimate the charge transfer in indium antimonite (InSb).

Keywords: Ionic model (IM), Compton profile (Cp), Indium Antimonite (InSb), Electron momentum density (EMD), LCAO method.

Received 27 November 2023; Accepted 12 February 2024.

Introduction

Group (III–V) materials such indium antimonite (InSb) demonstrate excessive promise such devices [1]. InSb takes the shape of zinc blend-structured dark grey metallic crystals. [2]. At 300K and 80K, respectively, InSb has narrow, straight and constricted band gaps of (0.17 eV) and (0.23 eV). For electrons, InSb has an extremely low effective mass of 0.014 m_e [2- 5] and a low density of conditions in the band of conduction. At ambient temperature, InSb tends to have the highest carrier mobility at $7.8x10^4$ cm^2/V.s. [6-7] Though InSb would have a reasonably great thermal conductivity of 20 Wm/k at 300K [8], it is not particularly low. Due to its low operating voltage of 0.5V, InSb would be a low-power semiconductor [7-9]. InSb is low-cost and available in market, also it provided in the form of bulk substrates and could be simply prepared in a high accuracy. The Zinc blende crystal structure Brillouin zone of InSb as given in Fig.1.

Due to the important of photo-electric characteristics and photovoltaic apps, InSb semiconductor is become significant and has been an important research topic for the last decades [10]. InSb has several uses in infrared detectors, thermal imaging cameras, and forward-looking infrared (FLIR) imaging systems. [7-11]. Photo diodes and quick transistors are used as thermal image detectors because of their vast carrier mobility [3–12]. When sandwiched among sheets of aluminum indium antimonite, it might additionally serve as a quantum well for other materials [13–14]. The best semiconductor for thermoelectric apps is InSb because it has the fastest carrier mobility among other semiconductors, the smallest effective mass of conduction electrons, and the lowest state density. Lately, InSb has focus on numerous theoretical and empirical studies on the establishment of various thermoelectric and opto-electric materials by making use of doping materials [7–15], various alloys, and nanostructures (nanowires)[3], in order to attain thermoelectric properties that are noticeably improved [16]. The study of electrical properties provides the foundation for understanding these characteristics, though. In the past, numerous methodologies have been used to study the electrical characteristics of InSb. These methods include the adiabatic logical density approximation (ALDA) [18], the experimental

pseudopotential approach [19], and the complete relativistic linear Mu n-tin-orbital method -LMTO [17]. In the inelastic process known as Compton scattering (CS), a powerful photon clashes with a solitary electron and gives some of its potential capability to the electron. This method was acknowledged as a potent and adaptable instrument of the experiment to test the uniformity for these models of the ground state of electron momentum density band structures. The Doppler widening of the scattered radiation caused by the velocity of the target's electrons serves as the foundation for Compton material studies [20, 21]. The electron momentum distribution, and therefore the E-structure of constituents, are reflected in the energy spectrum of elastically dispersed photons at fixed angles. The double differential cross-section, that is connected to the Compton profile $J(P_Z)$, may be measured from such tests as follows

$$J(P_Z) = \int_{P_x}^{\infty}\int_{P_y}^{\infty} \rho(\vec{p})\, dp_x dp_y \propto \frac{d^2\sigma}{d\Omega\omega_2} \qquad (1)$$

Here, $\rho(\vec{p})$ is the sample EMD of the electrons and is linked with functions of the real-space wave. ω_2 is the scattered photon energy and p_z the electron momentum (EM) component along the scattering vector direction (often as z-axis). The density of momentum within an independent-particle model is provided by

$$n(\boldsymbol{p}) = \frac{1}{(2\pi)^3}\sum_{Occ.}\left|\int \psi(\boldsymbol{r}) e^{(ip.r)} d\boldsymbol{r}\right|^2 \qquad (2)$$

In this equation, $\psi(\boldsymbol{r})$is the location seemed to be function for the e^- is the i^{th} state. and the summation expands across the entire occupied states.

The key aim of the current work is to (1) measure the pioneering Experimental Compton profiles(CP) of InSb by employing 59.54 keV Gamm-radiations, (2) compute the theoretical Compton profiles(CPs) of InSb by making use of density functional theory (DFT) represented in ab initio CRYSTAL-06code of Torino group. In this paper, all the quantities used are in atomic units (a.u.) with h = m = e = 1(a.u) and c = 137.036 (a.u), providing the unit momentum equl 1.9929×10^{-24} kg ms^{-1}, unit energy = 27.212 electron volt, and unit length equal 5.2918×10^{-11} meter.

I. Theory and Computational Methodology

1.1. The DFT-LCAO theory

In this theory, the method of *ab initio* linear combination of atomic orbitals (LCAO) is used in the program CRYSTAL06 [22]. Orbitals of crystal is enlarged as linear some combination of Bloch functions.

$$\varphi_{ik}(\mathbf{r}) = N\sum_{ji}^{m} a_{ji}(\mathbf{k})\sum_{g}\chi_{gi}(\boldsymbol{r})e^{(ik.g)} \qquad (3)$$

The Bloch functions of the local atom-centered Gaussian solves an equation from the next:

$$H_i\varphi_{ki}(r) = E_{ki}\varphi_{ki}(r) \qquad (4)$$

The current calculations using the LCAO-pseudopotential (PP) method may include an effective core pseudopotential (ECP), which assumes that the core electrons have a potential that is effectively averaged. The one-electron Hamiltonian includes operators for kinetic energy, Coulomb interaction, exchange-correlation, and effective core potential. The electronic structure of materials may be analysed using the pseudopotential (PP) framework, which incorporates both (HF) and (DFT) approaches. This includes hybrid approximations that integrate parts of both HF and Kohn-Sham Hamiltonians [23, 24]. The DFT include exchange-correlation potential operative regarding exchange-correlation energy is very per particle in the gas of the uniform electron [25]. The present calculations were performed for InSb crystal structure of Zinc-blende, which has an Indium atom at the origin (0, 0, 0) and an Antimony atom at (0.25, 0.25, 0.25). The crystalline form of InSb is created by XCrysden as illustrated in Fig. 1. Its lattice constants a = b = c = 6.48 Å and space group T^2_d _F_43 m [26-27]. The whole electron bases set for In and Sb were cited from http://www.tcm.phy.cam.ac.uk/basis_sets. After providing the default tolerances in the CRYSTAL06 code, the self-consistent field- SCF calculations were carried out for (29k-points) in the Brillouin Zone-BZ. The theoretical directional Compton profiles (CPs) were rendered to normal the equivalent free atom Compton profiles (CP) field.

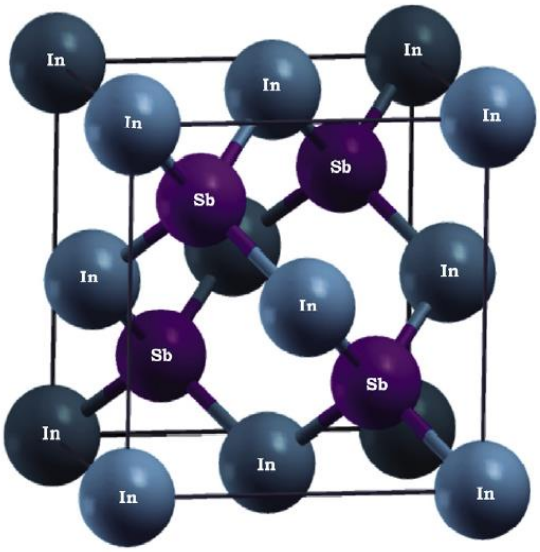

Fig. 1. Zinc blende structure of InSb.

1.2. Ionic Model (IM)

The free profiles related to the atom of In and Sb, acquired from Bigge et al. [21], were used to construct the theoretical (CP) of InSb for various ionic configurations. Shifting x- electrons from the 5p In shell to the 5P Sb shell allowed researchers to determine the valence profile for a variety of (In^{+x}) (Sb^{-x}) $(0.0 \le x \le 1.0)$ in the step of (0.25) combinations. The configurations for the core contributions of the (In^{+x}) (Sb^{-x}) valence profile was combined to get the overall profile. All of the profiles were properly normalized for comparation with other computations and the measurement.

II. The measurement and data analysis of the Compton profile(CP)

The Compton profile (CP) measurements were performed using the ^{241}Am γ-ray spectrometer that Sharma-et al. [28] described it. The sample of InSb scattered the incident gamma rays at an angle of 166±3.0^{o} from the 5 Ci annular ^{241}Am source, which had a gamma energy of 59.54 KeV. The scattering chamber was emptied to around (10-2) Torr using a rotating oil pomp to lessen the involvement of air scattering, as well as holding the sample vertically by attaching it to the rear of the lad-coated brass slab with a hollow that had a radius of 9.05 mm. A liquid nitrogen-cooled HPGe detector (Canberra type, GL110S), with a total resolution momentum of 0.6 a.u., was used to study the scattered radiation. By 4096 channels, a multichannel analyzer (MCA) used to record the spectra. Regarding momentum, the channel width was around (20) eV or (0.03) a.u. Measurements were made for 14 hours with an empty sample holder to account for the background. The observed background was then scaled to the actual counting time and removed channel by channel from the raw data. After that, the adjusted background spectra were subjected to several adjustments, including absorption of the sample, instrumental resolution, and cross section scattering, to produce the CP that employs computer code developed by the Warwick group [29–30]. After translating the profiles into the momentum scale, a MonteCarlo simulation was conducted to consider the various scattering corrections histories, which involved around 107 photons. The range of the rectification profile was standardized to 39.224 electrons or 0 to +7 a. u.

III. Results and discussion

The DFT-LCAO approach and the ionic model (IM) have been used to compute the Compton profiles (CPs). We have considered a variety of ionic configurations in the ionic model. (In^{+x}) (Sb^{-x}) ($0.0 \leq x \leq 1.0$) in step of 0.25. Table 1 provides the findings we found for theoretical and empirical Compton profiles. Columns 2 to 5 include the ionic profiles for a few ionic configurations. The empirical Compton profile (CP), which includes experimental faults at specific sites, is presented in the final column of the table. The theoretical Compton profile, which is not convoluted, spherically averaged, and stemmed from PBE correlation functional, is shown in column 6. The whole set of profiles will allow other workers to utilize them for experiments with varying momentum resolution. All theoretical profiles were convolved with a Gaussian function having a half maximum width (FWHM 0.6 atomic units in order to compute difference profiles for quantitative comparison represented in $\Delta J = J^{\text{Theory(pz)}} - J^{\text{Expt.(pz)}}$ The entire values were adjusted to be equivalent to 39.224 electrons with a range of momentum from 0 to +7 a.u. Fig 2 shows the difference curves that were subsequently produced from various ionic configurations. The ionic configuration with (x = 0.75) indicates the highest deviancy in respect to the experimentation conducted J(0), whereas this figure illustrates that the impact of charge moves from In to Sb,

Table1.

Ionic-IM , Unconvoluted theoretical data (DFT-LCAO and the experimental Compton profiles(Cps) of InSb. The whole profiles are rendered to normal to 39.224e^{-} from (0 to +7) a.u.
Statistical faults (±σ) are also provided at certain points. The entire profiles are in e.(a.u.)$^{-1}$

Pz (a.u.)	**J(Pz) e.(a.u.)$^{-1}$**					
	Ionic Model				**DFT-LCAO**	**Experiment**
	$In^{+0.25}Sb^{-0.25}$	$In^{+0.5}Sb^{-0.5}$	$In^{+0.75}Sb^{-0.75}$	$In^{+1}Sb^{-1}$		
0	18.054	18.756	18.999	18.799	22.655	17.694±0.062
0.1	17.876	18.502	18.750	18.550	22.391	17.693
0.2	17.347	17.784	18.034	17.850	21.656	17.367
0.3	16.482	16.678	16.909	16.776	20.555	16.746
0.4	15.415	15.405	15.592	15.527	19.235	15.931
0.5	14.289	14.151	14.282	14.277	17.685	15.034
0.6	13.241	13.054	13.129	13.162	15.811	14.116
0.7	12.370	12.185	12.215	12.264	13.744	13.198
0.8	11.667	11.512	11.507	11.559	11.825	12.300
1	10.657	10.571	10.528	10.569	9.559	10.739±0.055
1.2	9.929	9.886	9.830	9.860	8.728	9.760
1.4	9.266	9.240	9.183	9.206	8.153	9.267
1.6	8.585	8.561	8.509	8.529	7.555	8.901
1.8	7.881	7.855	7.809	7.827	6.937	8.603
2	7.178	7.149	7.108	7.124	6.309	8.051±0.045
3	4.423	4.403	4.381	4.390	3.896	4.157±0.032
4	3.098	3.089	3.07	3.082	2.810	2.623±0.025
5	2.448	2.444	2.437	2.440	2.300	2.278±0.02
6	1.999	1.997	1.993	1.995	1.923	1.926±0.018
7	1.635	1.633	1.632	1.632	1.595	1.674±0.013

which is significantly noticeable within the 0-3.0 a.u. momentum range (x = 0.5) is highly agreed upon. Away from 3.0 a.u., the entire curves of difference are identical since the role in this momentum area is controlled by those internal electrons that remain uninfluenced in the charge transference. To examine that the entire ionic configurations highly agreed with the experimentation, the entire range i.e., 0 to +7 a.u., has been calculated χ^2 and given as:

$$\chi^2 = \sum_{p_z}^{7.0} \left|\frac{\Delta J(p_z)}{\sigma(p_z)}\right|^2 \qquad (5)$$

where (p_z) stands for the consistent error of the experiment.

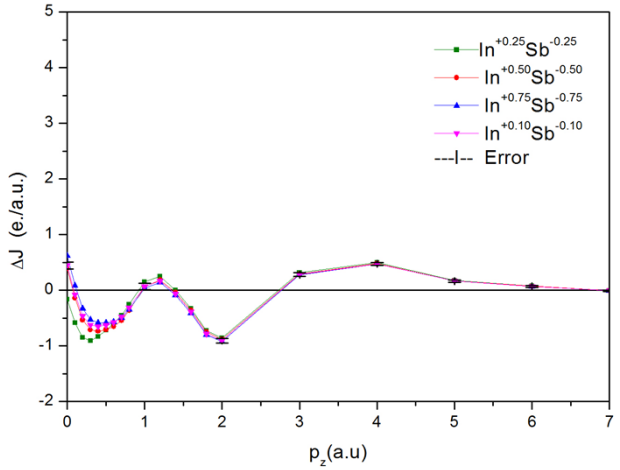

Fig. 2. The variation ΔJ among convoluted ionic and empirical CP of InSb. Empirical errors (±σ) are also illustrated at the points. Using a Gaussian width of 0.6 atomic units (FWHM)., the whole ionic profiles are convoluted together.

According to the χ^2 exam and Fig. 2, it is inferred that $In^{+0.5}Sb^{-0.5}$ configuration provides a highly agreed suggestion transfer of(0.5 e^-) from the valence 5p state of Is to the 5p state of Sb. Fig. 3 (a-upper panel) shows the absolute experimental, and (b-lower panel) presents the difference between theoretical (Ionic and DFT-PBE) and experimental momentum density of InSb. From the absolute curve, it is realized that at p_z = 0 a.u. The ionic (CP) is greater than the empirical and theoretical DFT-PBE Compton profiles.

To evaluate a quantitative comparison between experiment and theory, the difference profiles ($\Delta J = J^{Theory(pz)} - J^{Expt.(pz)}$) were obtained after convoluting the theoretical CP with the function of Gaussian 0.6 a.u. Here, the theoretical Compton profile (CP) is the sum of spherically averaged CP of valence electrons obtained using DFT-LCAO method and the core electrons from the free atom profile given by Biggs et al. [21]. This total theoretical Compton profile (CP) is then normalized to 39.224 electrons for InSb. It is examined that the difference curve shows close conformity with the experimental (CP) in the extra momentum region that is beyond p_z = 3 a.u. The reason behind this agreement is basically the contribution of core electrons that are defined very well via the free profiles of the atom. The difference curve exposes that the momentum density based on theory (Ionic model-IM and DFT-PBE) is smaller of the experimentation in the reduced momentum area ($0.0 \leq pz \leq 2.8$) a.u. The theoretical Compton profiles (CPs) (Ionic and DFT-PBE) are found to be larger than the experiment in the middle region, which is $2 \leq pz \leq 3.0$ a.u. The momentum density for the DFT-PBE is reported to be better agreed on with the experiment when compared to DFT-PBE configurations according to χ^2 values.

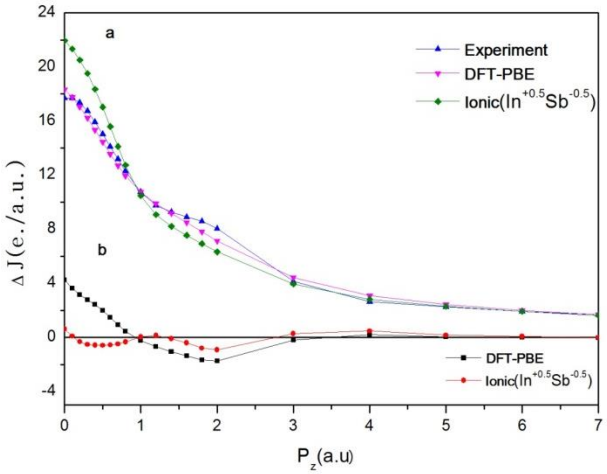

Fig. 3. (a) The absolute DFT-PBE, Experimental and Ionic (CPs) of InSb, (b) shows difference ($\Delta J = J^{Theory(pz)} - J^{Expt.(pz)}$) among convoluted theoretical and the empirical CP. Empirical errors (±σ) are indicated at certain points. The theoretical profile and the Gaussian are convoluted together with 0.6 a.u. FWHM.

Conclusion

To go over the main points, we have shown the E-structure and electron momentum density of InSb by making use of the Compton scattering method. The theoretical calculations are made by using LCAO method, and the values are contrasted with the experimental data. The obtained polycrystalline Compton data for InSb agrees well with the spherically averaged theoretical (Cps) calculated using the DFT-PBE technique. The momentum densities obtained with DFT-PBE and ionic configurations are underestimated by the experimental data in the reduced momentum region ($0 \leq p_z \leq 2.8$). The IM based computations were used to obtain the approximate charge transfer in the compound. As a results, IM had suggested that transferring of (0.5e^-) from 5p state of In to 5p state of Sb atom.

Sameen F. Mohammed – Doctor of Education, Department of Mechanical Techniques, Technical institute Kirkuk;
Mahmood A. Mohammed – MSc, Department of Mechanical Techniques, Technical institute Kirkuk.

[1] X. Zhang, Y. Hao, G. Meng, L. Zhang, *Fabrication of Highly Ordered InSb Nanowire Arrays by Electrodeposition in Porous Anodic Alumina Membranes*, Journal of The Electrochemical Society, 152, C664 (2005); http://dx.doi.org/10.1149/1.2007187.

[2] W. Liu, A.Y. Chang, R.D. Schaller, D.V. Talapin, *Colloidal InSb Nanocrystals*, Journal of the American Chemical Society, 134, 20258 (2012); https://doi.org/10.1021/ja309821j.

[3] M. I. Khan, X. Wang, K. Bozhilov, C.S. Ozkan, *Templated Fabrication of InSb Nanowires for Nanoelectronics*, Journal of Nanomaterials, 5, 698759 (2008); http://dx.doi.org/10.1155/2008/698759.

[4] K. Rahul, A.K. Verma, R.N. Tripathi, S.R. Vishwakarma, *Effect of substrate temperature on the electrical and optical properties of electron beam evaporated indium antimonide thin films*, Materials Science-Poland, 30 (4), 375 (2012); https://doi.org/10.2478/s13536-012-0044-x.

[5] F.W. Wise, *Lead Salt Quantum Dots: the Limit of Strong Quantum Confinement*, Accounts of Chemical Research, 33 (11), 773 (2000); https://doi.org/10.1021/ar970220q.

[6] D.L. Rode, *Electron Transport in InSb, InAs, and InP*, Physical Review B, 3, 3287 (1971); https//doi.org/10.1103/PhysRevB.3.3287.

[7] S. Yamaguchi, T. Matsumoto, J. Yamazaki, N. Kaiwa, A. Yamamoto, *Thermoelectric properties and figure of merit of a Te-doped InSb bulk single crystal*, Applied Physics Letters, 87 (20) 201902 (2005); http://dx.doi.org/10.1063/1.2130390.

[8] A.L. Miranda, B.Xu, O. Hellman, A.H. Romero, M.J. Verstraete, *Ab initio calculation of the thermal conductivity of indium antimonide*, Semiconductor Science and Technology M, 29 (12), 124002 (2014); https:///doi:10.1088/0268-1242/29/12/124002.

[9] R. Ahmed, Fazal-E-Aleem, S.J. Hashemifar, H. Rashid, H. Akbarzadeh, *Physical Properties of III-Antiminodes – a First Principles Study*, Communications in Theoretical Physics, 52 (3), 527(2009); https://doi.org/10.1088/0253-6102/52/3/28.

[10] S. Massidda, A. Continenza, A.J. Freeman, T.M. de Pascale, F. Meloni, M. Serra, *Structural and electronic properties of narrow-band-gap semiconductors: InP, InAs, and InSb*, Physical Review B, 41 12079 (1990); https://doi.org/10.1103/physrevb.41.12079.

[11] C.R. Bolognesi, D.H. Chow, Electron Device Letters, IEEE, *InAs/AlSb dual-gate HFETs*, 17 (11) 534 (1996); https://doi.org/10.1109/55.541772.

[12] P.E. Thompson, J.L. Davis, M.J. Yang, D.S. Simons, P.H. Chi, *Controlled p- and n-type doping of homo- and heteroepitaxially grown InSb*, Journal of Applied Physics 74 (11), 6686 (1993); https://doi.org/10.1063/1.355111.

[13] Y-S. Kim, M. Marsman, G. Kresse, F. Tran, P. Blaha, *Towards efficient band structure and effective mass calculations for III-V direct band-gap semiconductors*, Physical Review B, 82, 205212 (2010); http://dx.doi.org/10.1103/PhysRevB.82.205212.

[14] M. Razeghi, *High-power laser diodes based on InGaAsP alloys*,Nature 369 (6482), 631-633 (1994); https://doi.org/10.1038/369631a0.

[15] T. He, J. Chen, H.D. Rosenfeld, M.A. Subramanian, *Thermoelectric Properties of Indium-Filled Skutterudites*, Chemistry of Materials, 18 (3); 759 (2006); https://doi.org/10.1021/cm052055b.

[16] W.K. Liebmann, E.A. Miller, Preparation, *Preparation, Phase-Boundary Energies, and Thermoelectric Properties of InSb-Sb Eutectic Alloys with Ordered Microstructures*, Journal of Applied Physics, 34 (9), 2653 (1963); https:// doi:10.1063/1.1729786.

[17] M. Alouani, L. Brey, N.E. Christensen, *Calculated optical properties of semiconductors*, Physical Review B , 37 1167-1179(1988); https://doi.org/10.1103/physrevb.37.1167.

[18] A. De, C.E. Pryor, *Predicted band structures of III-V semiconductors in the wurtzite phase*, Physical Review B, 81 (2010); https://doi.org/10.1103/PhysRevB.81.155210.

[19] P.K. Joshi, D. Mali, K. Kumar, N.L. Heda, B.L. Ahuja, *High energy Compton scattering, electronic structure and optical response of zirconium substituted lead titanate*, Radiation Physics and Chemistry, 1991 10294 (2022); https://doi.org/10.1016/j.radphyschem.2022.110294.

[20] F. Biggs, L.B. Mendelsohn, J.B. Mann, *Hartree-Fock Compton profiles for the elements*, Atomic Data and Nuclear Data Tables, 16 (3), 201 (1975); https://doi.org/10.1016/0092-640X(75)90030-3.

[21] A.Yu. Kuznetsov, A.B. Sobolev, A.S. Makarov and A.N. Velichko, *First-principles calculations of the electronic structure and plastic properties of CsCl, CsBr, and CsI crystals*, Physics of the Solid State, 47, 2030 (2005); https:// doi.org/10.1134/1.2131140.

[22] R. Dovesi, V.R. Saunders, C. Roetti, et al., CRYSTAL06 User's Manual, University of Torino, Torino, 2006.

[23] A.D. Becke, *Density-functional exchange-energy approximation with correct asymptotic behavior*, Phys. Rev. A 38, 3098 (1988); https://doi.org/10.1103/PhysRevA.38.3098.

[24] S.F. Mohammed, F.M Mohammad, J. Sahariya, H.S. Mund, K.C. Bhamu, B.L. Ahuja, *Electronic structure of CaCO3: A Compton scattering study*, Applied Radiation and Isotopes, 72, 64 (2013); https://doi.org/10.1016/j.apradiso.2012.10.006.

[25] John P. Perdew, Kieron Burke, and Matthias Ernzerhof, *Generalized Gradient Approximation Made Simple*, Phys. Rev. Lett. 78, 1396 (1997); https://doi.org/10.1103/PhysRevLett.77.3865.

[26] B.L. Ahuja, F.M. Mohammad, S.F. Mohammed, H.S. Mund, N.L. Heda, *Compton scattering and charge transfer in Er substituted DyAl*, Journal of Physics and Chemistry of Solids, 7750 (2015); https://doi.org/10.1016/j.jpcs.2014.09.010.

[27] http://www.tcm.phy.cam.ac.uk/.
[28] B.K. Sharma, A. Gupta, H. Singh, S. Perkki◌, A. Kshirsagar, D.G. Kanhare, *Compton profile of palladium*, Physical Review B, 37, 6821 (1988); https://doi.org/10.1103/PhysRevB.37.6821.
[29] B. Williams, Compton Scattering, McGraw-Hill, London, 1977.
[30] F. Biggs, L.B. Mendelsohn, J.B. Mann, *Hartree-Fock Compton profiles for the elements*, 16201 (1975); https://doi.org/10.1016/0092-640X(75)90030-3.
[31] B.L. Ahuja , M. Sharma, *Performance of 20 Ci137Cs γ-ray Compton spectrometer for the study of momentum densities*, Pramana Journal of Physics, 65137 (2005); http://dx.doi.org/10.1007/BF02704383.

С.Ф. Мохаммед, М.А. Мохаммед

Дослідження електронної структури InSb: експеримет та теорія

Кафедра механічних технологій, Технічний інститут Кіркук, Північний технічний університет, Ірак, sameenmhammed@gmail.com

У дослідженні наведено результати, пов'язані із аналізом комптонівського розсіювання (Cs) антимоніту індію (InSb). Для експериментальних вимірювань використовується спектрометр Комптона 241Am з джерелом гамма-випромінювання 59,54 кеВ. Лінійна комбінація атомних орбіталей - метод LCAO використовується в рамках теорії функціоналу густини - DFT для оцінки теоретичних значень розподілу густини імпульсу електронів. Виконано порівняння результатів дослідження та емпіричними даними. Експериментальні ізотропні профілі виявилися узгодженими із даними DFT. Крім того, для оцінки перенесення заряду в антимоніті індію (InSb), розрахунки з використанням іонної моделі (IO) на основі 5p-стану In і 5p-стану атомів Sb показали, що 0,5 електроного 5p-стану In могло бути перенесено у 5p-стан атомів Sb.

Ключові слова: Іонна модель (IM), комптонівський профіль (Cp), антимоніт індію (InSb), густина імпульсу електронів (EMD), метод LCAO.